MATHEMATICAL BIOSCIENCES
AND ENGINEERING
Volume **12**, Number **5**, October **2015**

doi:10.3934/mbe.2015.12.907

pp. **907–915**

THERMAL DETECTION OF A PREVASCULAR TUMOR EMBEDDED IN BREAST TISSUE

Ephraim Agyingi, Tamas Wiandt and Sophia Maggelakis

School of Mathematical Sciences, Rochester Institute of Technology
Rochester, NY 14623-5603, USA

(Communicated by Heiko Enderling)

Abstract. This paper presents a mathematical model of heat transfer in a prevascular breast tumor. The model uses the steady state temperature of the breast at the skin surface to determine whether there is an underlying tumor and if so, verifies whether the tumor is growing or dormant. The model is governed by the Pennes equations and we present numerical simulations for versions of the model in two and three dimensions.

1. **Introduction.** Early detection of a breast tumor is critical in treating the disease. Among the diagnostic tools available, one is thermography which provides a temperature distribution of the breast region using an infrared camera. Thermography was approved in 1982 by the FDA as an adjunct procedure in the diagnosis of breast cancer [2]. The sensitivity of current infrared cameras has greatly increased since then and is such that temperature differences to 0.025°C can be detected [7]. As a consequence, temperature differences of 0.05 to 0.1°C can be reliably measured [12, 13].

Following Lawson's [16, 17] observations that the local temperatures of the skin over a tumor were significantly higher than normal skin, several numerical models have been developed that relate the skin temperature to the presence or absence of an underlying tumor [1, 8, 9, 12, 13, 19, 18, 20, 22, 24]. Of particular interest is the model by Maggelakis et al [19] which is distinct from others in that it focuses on a prevascular tumor. This is a tumor that is yet to be connected to the host capillary network and obtains nourishment exclusively through diffusion from neighboring healthy tissues. The tumor is solid and consists of a necrotic core surrounded by a region of proliferating cells. Folkman [10] established that such tumors can be dormant for a very long time and in the process attain a maximum diameter of about 1mm before being vascularized.

It is known that various human organs harbor prevascular tumors throughout their life span [5, 11]. Most of these tumors are usually arrested at the prevascular stage due to metabolic restrictions. Examples of tumors that present at depths very close to the surface of the breast are Paget disease of the breast, male breast cancer, lipoma of the breast, fat necrosis of the breast, and melanoma, among others. Detecting a prevascular tumor that has the potential of becoming malignant provides an excellent chance to eradicate the disease.

2010 *Mathematics Subject Classification.* Primary: 80A20, 92C05; Secondary: 92C30.
Key words and phrases. Heat transfer, prevascular tumor, temperature distribution.

The published literature on models and simulations of heat transfer in breast tumors focuses primarily on vascularized tumors. The models are all governed by the Pennes bio-heat equation. Mital et al.[20] developed and tested a thermographic procedure for estimating the location and power of an embedded heat source. They simulated a tumor in biological tissue by conducting an experiment where a resistance heater was embedded in agar. The surface temperature profile was obtained with an infrared camera and using a genetic algorithm that solves the Pennes equation they accurately estimated the location and the heat generation rate of the source.

Paruch et al.[22] carried out a simulation study in which they simultaneously solved inverse problems to estimate the thermal conductivity, the perfusion coefficient, the metabolic heat generation rate, and the location and size of the tumor region assuming the skin surface temperature is known. Lin et al.[18] considered a small breast tumor 12mm in diameter at depths $20 - 50.8$mm from the nipple tip. Using a technique that enhances the thermal signature of the tumor, it was shown that the thermal characteristic of an embedded small tumor even in deeper regions can be captured. Their results were obtained by setting the metabolic heat generation in the tumor region at 24.156W/cm^3 (which is about 2500-5000 times the metabolic heat generation rates of normal tissue).

In [13], González used a fixed metabolic heat generation value for the tumor to show that infrared cameras can detect breast tumors as small as 0.5cm at a depth of 2cm. In his more recent work [12] of estimating the metabolic heat generation of breast tumors indirectly and noninvasively using digital infrared images, it was found that tumors present very wide ranges of metabolic heat generation values. Of the 20 patients involved in the study with breast tumors of sizes $1 - 10$cm, at depths of $0.5 - 2.6$cm, 14 patients had tumors with metabolic heat generation in the range $.205 - 1.645\text{W/cm}^3$ (which is about 20-200 times the metabolic heat generation rates of normal tissue).

Models on the growth of solid tumors (also known as spheroids) that relate the viable region to the necrotic core do appear in the literature [14]. Mueller-Klieser [21] derived a simple model for spheroids and demonstrated by measurement that the necrotic core was quite substantial. In a more recent work by Grimes et al [15], which expands on the results in [21], an explicit formula that relates the oxygen consumption rate of the spheroid to the radius of the necrotic core is provided. As a consequence, an estimate of the viable volume of a tumor that is generating heat can be predetermined.

It is well established that heat transfer away from a tumor is dependent on perfusion and that as the the perfusion rate decreases the tumor temperature increases [4]. Further, any change in temperature between normal and tumor tissue is characterized by conduction and convection between the two tissues. Observing that prevascular tumors are small (about 1mm in diameter), and have no vasculature linking them to their microenvironment, this paper's aim is the study of heat transfer in these tumors. The work reported here builds on the one-dimensional model provided in [19]. We employ a basic numerical approach that captures the dominant effects in the heat transfer of the tumors, while ignoring the insignificant complicating details present in the true biological condition. The paper is organized as follows: in Section 2, we provide a mathematical model based on the Pennes bioheat equation; in Section 3, results and discussions using different parameters of the model are presented; and finally concluding remarks are provided in Section 4.

2. **Mathematical model.** We investigate the problem of heat transfer in tumors; we are considering prevascular cancer cells located in the dermis. Extending the ideas presented in [19], we describe a mathematical model of heat transfer in a two-dimensional prevascular tumor. The goal is to provide a description of the conditions under which skin temperature is a good indicator of the presence of these tumors. We study the effects of tumor location, size, and grouping on the surface temperature.

Following [19], we consider prevascular cancer cells cultures located in the dermis. The heat flow in this region is described by the Pennes equation [23]

$$\rho\bar{c}\frac{\partial T}{\partial t} = \nabla\cdot(K\nabla T) + m_b c_b(T_A - T) + S,$$

where ρ is the tissue's density, $\bar{c}$ is the tissue's specific heat, K is the tissue's thermal conductivity, m_b is the mass flow rate of blood, c_b is the blood's specific heat, T_A is the arterial blood temperature, and S is the metabolic heat generation. We assume that the tumor is in the prevascular stage, thus the perfusion terms vanish and we obtain

$$\rho\bar{c}\frac{\partial T}{\partial t} = \nabla\cdot(K\nabla T) + S.$$

We will consider a two dimensional section of the dermal tissue, with the circular shaped tumor located in the subcutaneous region. The temperature of the dermis will be given by $T(x,y)$, where the x coordinate is the horizontal direction and y is the depth. At steady state, the time derivative is zero and the temperature $T_h(x,y)$ of the healthy tissue satisfies the equation

$$\Delta T_h = -\frac{S_h}{K_h},$$

where S_h is the metabolic heat generation of the healthy tissue and K_h is its thermal conductivity. We place the two dimensional cut in the (x,y)-plane such that the $y=0$ level corresponds to the bottom layer of the skin, and $y=d$ corresponds to the surface. We place the origin so that $-a \le x \le a$. The center of the tumor is at $(0,d/2)$, and its radius is R. Similarly to healthy tissue, at steady state, the temperature $T_t(x,y)$ of the tumor satisfies

$$\Delta T_t = -\frac{S_t}{K_t},$$

where S_t is the metabolic heat generation of the tumor and K_t is its thermal conductivity.

The corresponding boundary conditions will be given by

(i) $T_h(x,0) = T_b$ is the temperature of the body.

(ii) At the skin surface $(y=d)$, $-K\dfrac{\partial T_h}{\partial y} = \lambda(T_h - T_a)$, where T_a is the ambient temperature and λ is the surface heat transfer coefficient.

(iii) $T_h(-a,y) = T_h(a,y)$ is the temperature distribution of healthy tissue. The explicit computation for the value of this temperature distribution follows shortly.

(iv) We assume that the temperature is continuous across the interface of the healthy tissue and the tumor, i.e. $T_h(x,y) = T_t(x,y)$ when $x^2 + (y-d/2)^2 = R^2$.

(v) The heat flux is continuous across the interface of the healthy tissue and the tumor, i.e. $K_t\nabla T_t = K_h\nabla T_h$ when $x^2 + (y-d/2)^2 = R^2$.

The temperature distribution of healthy tissue can be computed, because the homogeneity of the tissue in this case reduces our problem to a one-dimensional equation of the form $\Delta T_h(x,y) = T_h''(y) = -\dfrac{S_h}{K_h}$, where y is the tissue depth, $T_h(0) = T_b$, and $T_h'(d) = -\lambda(T_h - T_a)/K$. The solution of this equation is given by

$$T_h(y) = -\frac{S_h}{K_h}\frac{y^2}{2} + \frac{S_h d - \lambda(-\frac{S_h}{K_h}\frac{d^2}{2} + T_b - T_a)}{K_h + \lambda d} y + T_b.$$

3. **Results and discussion.** The numerical simulations presented in this paper were performed using PDETOOL, a MATLAB finite element package. The following thermophysical parameter values, chosen to be consistent with Maggelakis et al [19], were used in our numerical computations: $S_h = 0.009\text{W}/(\text{cm})^3$, $K_h = K_t = 0.0042\text{W}/((\text{cm})^\circ\text{C})$, $\lambda = 0.0005\text{W}/((\text{cm}^2)^\circ\text{C})$. On the skin surface we assume a temperature of $T_a = 23^\circ$C and on the internal boundary at a depth $d = 0.5$cm below the surface, we assume a temperature of $T_b = 37^\circ$C. The axial parameter value is set at $a = 1$cm. In addition to these, other parameters were chosen to explore the behavior of the model as shown in the results below.

We note that only the outer shell of the tumor is producing heat. Using the formula provided in [21], we calculated the radius of the necrotic core of a spheroid of radius 0.1cm to be about 715μm and assumed that 50% of the total tumor volume was generating heat.

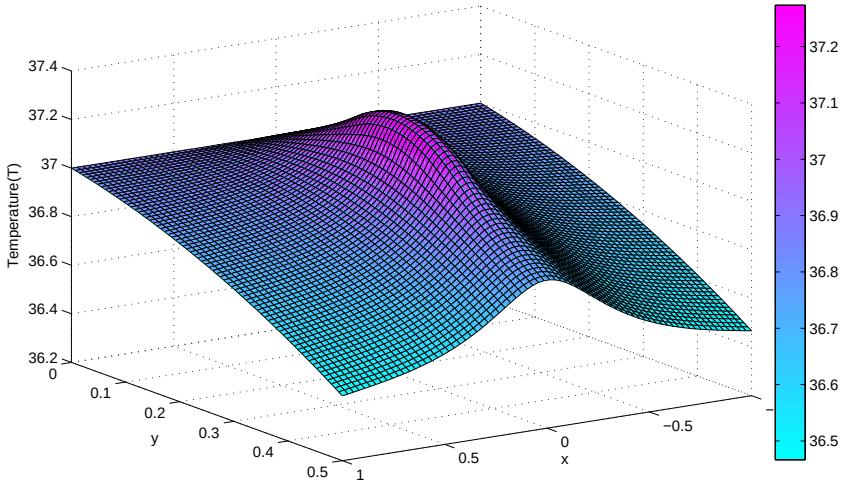

FIGURE 1. Temperature distribution across the entire domain for a tumor of radius $r = 0.1$cm, and $S_t = 0.18\text{W}/(\text{cm})^3$.

Figure 1 presents the steady-state temperature distribution over the whole domain for a spherical tumor of radius 0.1cm. The metabolic heat generation rate of the tumor was set at 20 times that of the normal breast tissue. The temperature starts with 37°C at the internal boundary and decreases towards the skin surface. The highest temperature in the entire domain is located in the region containing

the tumor. This is evident from Figure 1 if we consider any temperature profile through the center of the tumor.

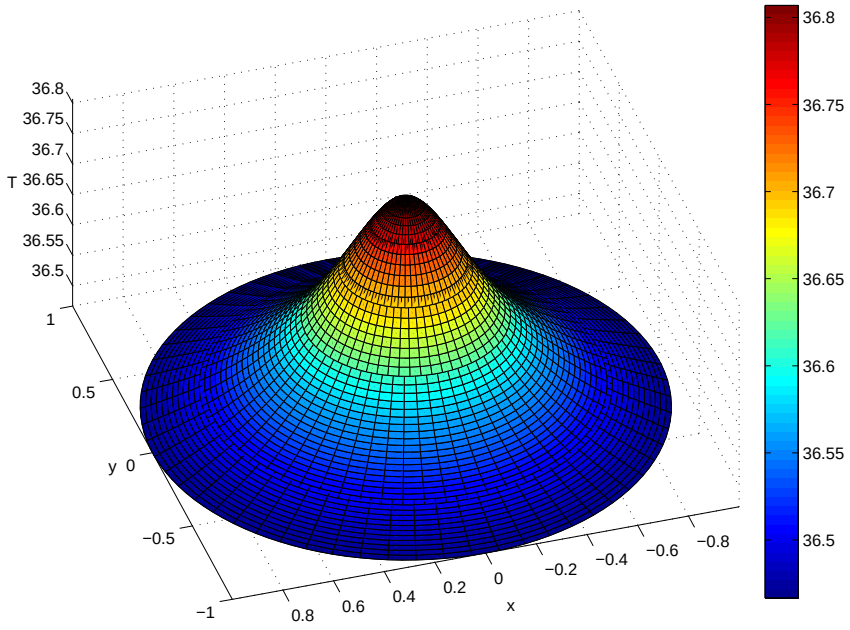

FIGURE 2. Temperature distribution skin surface for a tumor of radius $r = 0.1$cm, and $S_t = 0.18\text{W}/(\text{cm})^3$.

It is important that results from the model be easily related to those obtained from a thermal imaging device. Though the model was initially formulated in two dimensions, by assuming a cylindrical region with diameter $2a$ cm and height 0.5cm in which any vertical cross-section through the center yields our original domain, we extrapolated three-dimensional results as shown in Figure 2. It can be seen that the temperature at the skin surface is about 0.3°C higher than that of the surrounding region. Further, this result is important in tumor identification because we can deduce a two dimensional contour map from it that is similar to a thermal map from an imaging device.

In Figure 3, we present steady state temperature profiles at the skin surface for tumors of different sizes, with the same metabolic heat rate. We observe that the temperature flux at the skin surface is higher with an increase in radius. The implications of these results are useful in monitoring whether an identified tumor is dormant and harmless or expanding in size which points to the possibility of it becoming angiogenic.

Next, Figure 4 presents steady state surface temperature calculations for a tumor whose center is located at different depths. We see that the closer the tumor is to the surface, the higher the temperature output. The implication here is that a tumor closer to the skin surface will generate a better temperature contrast that can help identify them compared to ones located deep beneath the surface.

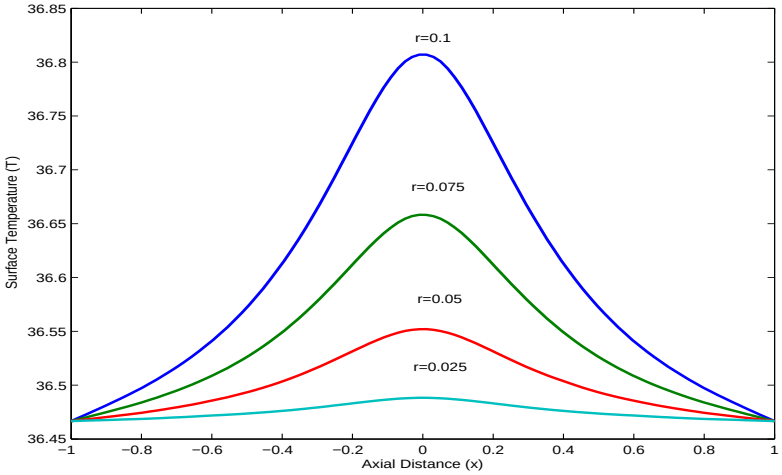

FIGURE 3. Skin surface temperature for different tumor sizes with $S_t = 0.18\text{W}/(\text{cm})^3$.

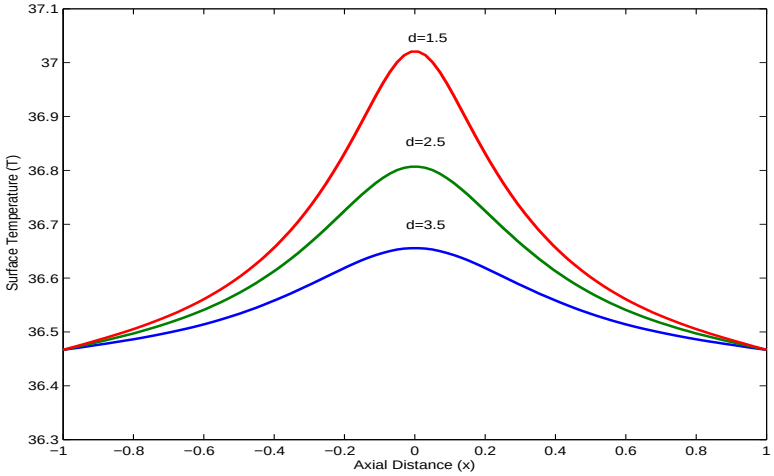

FIGURE 4. Skin surface temperature for a tumor of radius $r = 0.1\text{cm}$, and $S_t = 0.18\text{W}/(\text{cm})^3$ at different depths.

In our next result, Figure 5, we consider a tumor at the same location with different metabolic heat generating rates. The temperature profiles shown are for a tumor with metabolic heat generating rates that are two, ten and twenty times that of a healthy breast tissue. It is evident that the larger the metabolic rate, the greater the steady state temperature distribution at the skin surface. If we associate malignity with metabolic heat rate generation, then our results suggest that skin

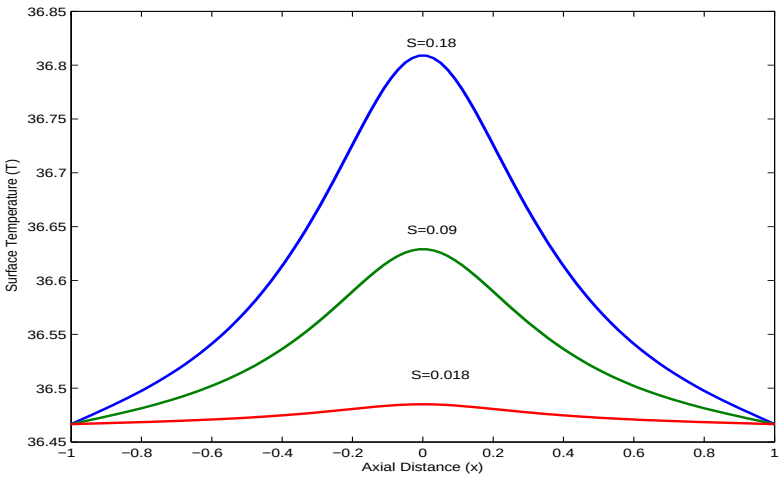

FIGURE 5. Skin surface temperature for a tumor of radius $r = 0.1$cm and different metabolic heat generating rates ($S = S_t$).

surface temperatures can be use to study the aggressive nature of an identified tumor.

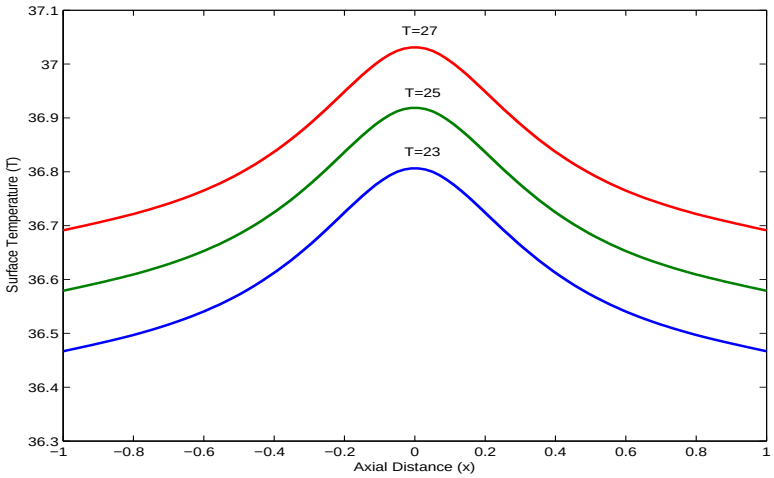

FIGURE 6. Skin surface temperature for a tumor with different ambient temperatures ($T = T_a$).

Figure 6 investigates the effect of different ambient temperatures at the skin surface. It can be seen that the higher the ambient temperature, the higher the steady state temperature of the skin. Comparing any two given profiles, the temperature differences are almost constant throughout the axial domain. This suggest that a

change in the ambient temperature does not alter the sensitivity of the thermography. It is only important that the ambient temperature be uniform over the entire skin surface that needs a temperature map.

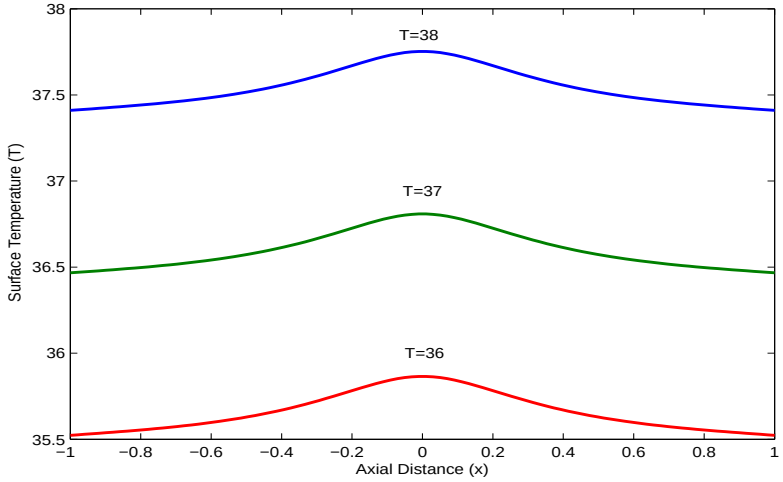

FIGURE 7. Skin surface temperature for a tumor with different internal body temperatures ($T = T_b$).

Finally, Figure 7 considers the intra-personal variation of human body temperature which is known to vary by $0.8 - 1^{\circ}$C [3]. The numerical results show that variations in the internal body temperature do not effect the sensitivity of the model.

4. **Conclusion.** In this paper, we have formulated a mathematical model of a prevascular breast tumor in two dimensions based on the Pennes bio-heat transfer equation. The effect of the tumor size, depth of tumor below skin surface, tumor metabolic heat generation and surrounding ambient temperature were investigated. Numerical simulations show that all these factors determine the steady state temperature distribution at the skin surface. Using symmetry, we easily deduced a three-dimensional result for a restricted problem whose contour map can be directly compared to that from an imaging device. Our results are consistent with many of the results reported in the literature for vascularized tumors and thus serve as additional tools in the fight against the disease.

The findings of this paper are limited in that they only apply to prevascular tumors that occur at depths very close to the surface of the breast.

REFERENCES

[1] J. P. Agnelli, A. A. Barrea and C. V. Turner, Tumor location and parameter estimation by thermography, *Mathematical and Computer Modelling: An International Journal*, **53** (2011), 1527–1534.

[2] N. Arora, D. Martins, D. Ruggerio, E. Tousimis, A. J. Swistel, M. P. Osborne and R. M. Simmons, Effectiveness of a noninvasive digital infrared thermal imaging system in the detection of breast cancer, *The American Journal of Surgery*, **196** (2008), 523–526.

[3] F. C. Baker, J. I. Waner, E. F. Vieira, S. R. Taylor, H. S. Driver and D. Mitchell, Sleep and 24 hour body temperatures: A comparison in young men, naturally cycling women and women taking hormonal contraceptives, *The Journal of Physiology*, **530** (2001), 565–574.
[4] G. F. Baronzio, A. Gramaglia, A. B. Baronzio and I. Freitas, *Influence of Tumor Microenvironment on Thermoresponse: Biologic and Clinical Implications,* Madame Curie Bioscience Database . Austin (TX): Landes Bioscience, 2000.
[5] W. C. Black and H. G. Welch, Advances in diagnostic imaging and overestimations of disease prevalence and the benefits of therapy, *New England Journal of Medicine*, **328** (1993), 1237–1243.
[6] M. Brennan and N. Houssami, Thermography in breast cancer diagnosis, screening and risk assessment: systematic review, *Breast Cancer Management*, **2** (2013), 163–172.
[7] J. D. Bronzino, *Medical Devices and Systems. Boca Raton*, FL:CRC/Taylor & Francis; 2006.
[8] C. K. Charny, Mathematical models of bioheat transfer, in *Bioengineering Heat Transfer*(ed. Y. I. Cho), Academic Press, (1992), 19–151.
[9] Z. Deng and J. Liu, Mathematical modeling of temperature mapping over skin surface and its implementation in thermal disease diagnostics, *Computers in Biology and Medicine*, **34** (2004), 495–521.
[10] J. Folkman, Tumor angiogenesis: Therapeutic implications, *New England Journal of Medicine*, **285** (1971), 1182–1186.
[11] J. Folkman and R. Kalluri, Cancer without disease, *Nature*, **427** (2004), p787.
[12] F. J. González, Thermal simulation of breast tumors, *Revista Mexicana de Fisica*, **53** (2007), 323–326.
[13] F. J. González, Non-invasive estimation of the metabolic heat production of breast tumors using digital infrared imaging, *QIRT Journal*, **8** (2011), 139–148.
[14] H. P. Greenspan, Models for the growth of a solid tumor by diffusion, *Studies in Applied Mathematics*, **LI** (1972), 317–340.
[15] D. R. Grimes, C. Kelly, K. Bloch and M. Partridge, A method for estimating the oxygen consumption rate in multicellular tumour spheroids, *Journal of the Royal Society Interface*, **11** (2013), p1124.
[16] R. N. Lawson, Implications of surface temperatures in the diagnosis of breast cancer, *Canadian Medical Association Journal*, **75** (1956), 309–310.
[17] R. N. Lawson and M. S. Chugtai, Breast cancer and body temperatures, *Canadian Medical Association Journal*, **88** (1963), 68–70.
[18] Q. Y. Lin, H. Q. Yang, S. S. Xie, Y. H. Wang, Z. Ye and S. Q. Chen, Detecting early breast tumour by finite element thermal analysis, *Journal of Medical Engineering & Technology*, **33** (2009), 274–280.
[19] S. A. Maggelakis and A. E. Savakis, Heat transfer in tissue containing a prevascular tumor, *Applied Mathematics Letters*, **8** (1995), 7–10.
[20] M. Mital and E. P. Scott, Thermal Detection of Embedded Tumors Using Infrared Imaging, *Journal of Biomechanical Engineering*, **129** (2006), 33–39.
[21] W. Mueller-Klieser, Method for the determination of oxygen consumption rates and diffusion coefficients in multicellular spheroids, *Biophysical Journal*, **46** (1984), 343–348.
[22] M. Paruch and E. Majchrzak, Identification of tumor region parameters using evolutionary algorithm and multiple reciprocity boundary element method, *Engineering Applications of Artificial Intelligence*, **20** (2007), 647–655.
[23] H. H. Pennes, Analysis of tissue and arterial blood temperatures in the resting forearm, *J. Appl. Physiol*, **1** (1948), 93–122.
[24] N. M. Sudharsan, E. Y. K. Ng and S. L. Teh, Surface Temperature Distribution of a Breast With and Without Tumour, *Computer Methods in Biomechanics and Biomedical Engineering*, **2** (1999), 187–199.

Received January 28, 2015; Accepted April 22, 2015.

E-mail address: eoasma@rit.edu
E-mail address: tiwsma@rit.edu
E-mail address: sxmsma@rit.edu